Antibody Therapeutics, 2022, Vol. 5, No. 3 ***211–215***
https://doi.org/10.1093/abt/tbac018
Advance Access Publication on 10 August 2022

Brief Report

Use of Debye–Hückel–Henry charge measurements in early antibody development elucidates effects of non-specific association

Joshua R. Laber[1], Thomas M. Laue[2] and Dana I. Filoti[3,*]

[1]Formulation and Biologics Product Development, Nektar Therapeutics, 455 Mission Bay Boulevard South, San Francisco, CA 94158, USA , [2]Carpenter Professor Emeritus, University of New Hampshire, Durham, NH 03824, USA , and [3]Analytical Research and Development, AbbVie, 100 Research Drive, Worcester, MA 01605, USA

Received: January 10, 2022; Revised: June 21, 2022; Accepted: July 10, 2022

ABSTRACT

The diffusion interaction parameter (k_D) has been demonstrated to be a high-throughput technique for characterizing interactions between proteins in solution. k_D reflects both attractive and repulsive interactions, including long-ranged electrostatic repulsions. Here, we plot the mutual diffusion coefficient (D_m) as a function of the experimentally determined Debye–Hückel–Henry surface charge (Z_{DHH}) for seven human monoclonal antibodies (mAbs) in 15 mM histidine at pH 6. We find that graphs of D_m versus Z_{DHH} intersect at $Z_{DHH,} \sim 2.6$, independent of protein concentration. The same data plotted as k_D versus Z_{DHH} show a transition from net attractive to net repulsive interactions in the same region of the Z_{DHH} intersection point. These data suggest that there is a minimum surface charge necessary on these mAbs needed to overcome attractive interactions.

Statement of Significance: Within the protein electrostatics framework, a unique discussion is being carried out to depict the thermodynamic and hydrodynamic contributions to k_D via a novel model using the diffusion coefficient as a function of Debye–Hückel–Henry surface charge (Z_{DHH}). This work is a guide for protein engineering towards more developable mAbs.

KEYWORDS: antibody developability; surface charge; colloidal interactions; dynamic light scattering; diffusion interaction parameter

INTRODUCTION

Despite decades of research, the relationship between the colloidal stability of protein solutions at high concentrations and pairwise protein–protein interactions is still not well understood [1, 2]. Part of the problem is that the bulk of this research has been done using globular proteins such as bovine serum albumin [3], α-chymotrypsinogen A [4], ovalbumin [5], and lysozyme [6]. However, further investigation on this relationship is needed for the more asymmetric, therapeutically relevant monoclonal antibodies (mAbs) [7].

The diffusion interaction parameter (k_D), measured using dynamic light scattering (DLS), is a high-throughput, plate-based technique for characterizing protein interactions. In various low ionic strength buffer conditions, good correlation is observed between k_D with both viscosity [8] and accelerated storage stability of mAbs [9].

k_D is calculated from Equation 1, where the mutual diffusion coefficient (D_m) is measured as a function of protein concentration, c. The linear fit of the data yields the self-diffusion coefficient (D_s) from the intercept at $c = 0$ and yields the k_D from the slope [10].

$$D_m = D_s\,(1 + k_D c) \tag{1}$$

k_D depends on both the thermodynamics (k_T) of the protein–protein interactions and the diffusion hydrodynamics

*To whom correspondence should be addressed. Dana I. Filoti, AbbVie Bioresearch Center, 100 Research Drive Worcester, MA 01605, USA. Tel: +1-603-531-8051; Email: dana.filoti@abbvie.com

(k_H, equal to k_S in sedimentation) as shown in Equation 2.

$$k_D = k_T - k_H \tag{2}$$

$$k_D = 2M_w B_{22} - (\xi_1 + \nu_{sp}) \tag{3}$$

Equation 3 shows the explicit form for both k_T ($2M_wB_{22}$) and k_H ($\xi_1 + \nu_{sp}$), where M_w is the molecular weight, B_{22} is the second virial coefficient, ν_{sp} is the protein partial specific volume, and ξ_1 is the first-order coefficient of the virial expansion of the friction factor with protein concentration [10]. B_{22} is made more positive with increasing excluded volume and increasing charge–charge repulsion. Any attractive interaction, including mass action association, will decrease B_{22}; hence, decrease k_D. ξ_1 depends directly on the solution viscosity and is sensitive to the size and shape of the protein. Any attractive interactions between molecules increases ξ_1, thereby decreasing k_D. Notice then that k_D is always decreased by attractive energies between proteins.

At the protein concentrations used in this study, only bimolecular interactions will contribute significantly to k_D. The charge–charge repulsion contribution to k_D will be greatest at low salt conditions. Thus, it is anticipated that k_D will be greater at low salt than at high salt concentrations. Electrostatic interactions that are attractive in nature (e.g. charge-dipole) are less affected by salt than interactions that are repulsive in nature (e.g. charge–charge), thus these attractive interactions become more evident at higher salt concentrations [11, 12]. Because both k_T and k_H are positive values, positive values of k_D necessarily indicate the repulsive contributions to k_T (charge and excluded volume) to dominate over any attractive energy.

We have measured the Debye–Hückel–Henry surface charge (Z_{DHH}) for a set of seven mAbs with diverse isoelectric points (pIs of 8.5 ± 2) and measured D_m to obtain k_D values using DLS. We find graphs of D_m versus Z_{DHH} for the mAbs intersect at a single value of Z_{DHH} of ~2.6. Correspondingly, values of k_D cross over from negative to positive over this same narrow range. We propose that the Z_{DHH} of 2.6 represents the minimum protein surface charge to overcome attractive interactions.

MATERIALS AND METHODS

Monoclonal antibodies

The seven monoclonal antibodies used in this study have been produced by AbbVie and were IgG1s and chosen to be included in this study based on their pre-formulation developability screening assessment and their differing calculated isoelectric points (pIs of 8.5 ± 2). All seven of these mAbs experienced different levels of Chemistry, Manufacturing and Controls (CMC) development. The heavy chain isotype was either IgG1 or IgG2 and was combined with either a κ or λ light chain.

DLS

Concentrated protein stocks were thawed benchtop from −80°C and buffer exchanged into 15 mM histidine, 100 mM KCl, pH 6.0 using overnight dialysis against 5 L of buffer. Protein solutions were made between 2 and 12 mg/mL and concentration checked on a Thermo Scientific Nanodrop One (Waltham, MA). After passing thorough a 0.22 μm sterile filtration using Corning Costar Spin-X centrifuge tube filters (Salt Lake City, UT) at 1000×g, the diffusion coefficients of the proteins in the solutions were then run on a Malvern Zetasizer Nano ZS (Malvern, Worcestershire, UK) in triplicate.

Membrane-confined electrophoresis

Proteins were buffer exchanged into 15 mM histidine, 100 mM KCl, pH 6 via overnight dialysis against 5 L of buffer. After concentration check and dilution to 2 mg/mL, the Debye–Hückel–Henry surface charge was measured in triplicate in a steady state method (50, 75, and 100 μA) using the membrane-confined electrophoresis (MCE) instrument (Spin Analytical, Berwick, ME). The absorbance traces as a function of time were analyzed in the provided software as instructed by Spin Analytical.

Data and structure modeling

Calculated surface charge values at pH 6 were generated using Chemical Computing Group's MOE 2016.0802 software (Montreal, Canada). DLS diffusion data were analyzed and graphed in MATLAB (Mathworks, Natick, MA).

RESULTS AND DISCUSSION

The measured Debye–Hückel–Henry charge is different than the calculated surface charge

A growing body of literature has already described the dominant role that protein surface electrostatics has on protein–protein interactions, determined by measurements such as B_{22} or k_D [8, 10, 13, 14]. Here, we investigated the relationship between k_D and the Debye–Hückel–Henry surface charge (Z_{DHH}) [15] for a set of seven therapeutically relevant mAbs. These mAbs were chosen for their diverse isoelectric points and thus for their surface charges in 15 mM histidine buffer at pH 6, to reflect the suitability to be a development platform approach. For same pH 6 conditions, Figure 1 shows for each mAb the measured Z_{DHH} by using MCE compared with the theoretical surface charge calculated by MOE. As described in the Methods section, the MCE measurement of Z_{DHH} includes 100 mM KCl. Z_{DHH} is a system property that depends on pH and salt concentration [15]; however, the changes in Z_{DHH} over the salt concentration range used here (< 100 mM) are small (TL, personal observation). The seven mAbs have measured Z_{DHH} values between 0.9 and 11.1, whereas the calculated surface charges spans from 9 to 44. The substantial difference between the calculated charge and Z_{DHH} is primarily a consequence of anion binding [15–17].

Concentration dependence of D_m reveals protein and ionic strength differences in k_D

Figure 2 shows the dependence of D_m as a function of protein concentration for each of the mAbs. In Figure 2A

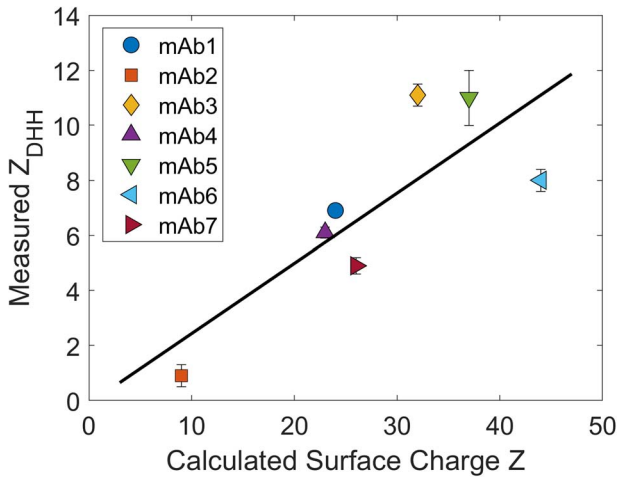

Figure 1. Comparison of the measured ZDHH and the calculated surface charge at pH 6 for the seven mAbs. Charge was measured in the pH 6.0 buffer containing 100 mM KCl. Error bars shown represent the standard deviation of at least three ZDHH measurements on the MCE. Calculated surface charge was obtained through structure-based modeling at pH 6 on MOE, as described in the Materials and Methods section. The calculations were made for solvent without 100 mM KCl. Shifts in the side chain pKas would result from added salt, but the changes to the calculated charge would be small. The solid black line representing the linear correlation between measured and calculated values has a slope of 0.26, intercept of −0.20, and an R^2 of 0.64.

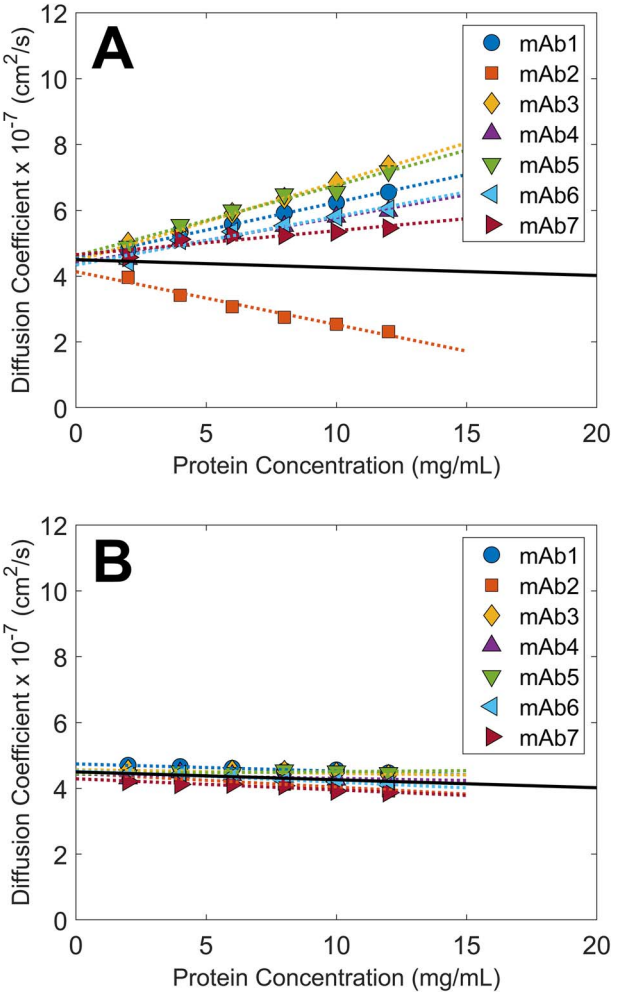

Figure 2. The diffusion coefficient concentration dependence measured at low and high ionic strength. The slope of each graph is kD as in (A) 15 mM histidine, pH 6 and (B) 15 mM histidine, 100 mM KCl, pH 6. At low ionic strength all the mAbs tested except one were observed to have repulsive interactions (kD > 0), whereas in 100 mM KCl the concentration dependence of the diffusion coefficients collapsed to a single line for all, close to the value of −5.34 mL/g (shown by the solid black line) indicating only excluded volume repulsive interactions.[5]

it can be seen that each mAb exhibits a unique slope, where increased slopes generally correlate with increased values of Z_{DHH} (Fig. 1). The slope of these lines in Figure 2 is k_D. Although there are considerable differences in the slopes at low ionic strength (Fig. 2A), the curves collapse to a much narrow range of slopes at high ionic strength (Fig. 2B). The decreased slopes at higher ionic strength are anticipated by the decreased charge–charge repulsion [11]. Indeed, the slope for all mAbs in Figure 2B is indistinguishable from that anticipated for mAbs exhibiting only excluded volume repulsion, −5.34 mL/g [7].

The near identity of k_D in high salt suggests that, for these mAbs, bimolecular interactions are dominated by charge–charge repulsion in low salt, which is overcome by Debye–Hückel screening at higher salt. This dominance of electrostatics at low mAb concentrations is in good agreement with previous work [8, 13]. Very weak self-association has been observed for mAbs which is hypothesized to be important for effector function [18, 19]. However, the effects of self-association only become apparent at concentrations far higher than those used here. Although there are examples of proteins that undergo significant changes in self-interaction properties as a function of pH, these proteins undergo pH-dependent enzymatic cleavage [20].

D_m and k_D dependence on Z_{DHH}

With an accurate value of Z_{DHH} and k_D for the different mAbs, the relationship between the diffusion parameters (D_m and k_D) and Z_{DHH} was investigated. For this analysis, values of Z_{DHH} act as stand-ins for the different mAbs. Figure 3A shows the correlation of D_m with Z_{DHH} in 15 mM histidine buffer at pH 6. For each mAb (i.e. each value of Z_{DHH}), the concentration dependence of D_m for that mAb is graphed at the Z_{DHH}. For each protein concentration, values of D_m vs. Z_{DHH} fit well to a general logarithmic function ($D_m = a^* ln(b^* Z_{DHH})$, where a and b are the constants) with all curves having $R^2 > 0.97$. Strikingly, independent of the protein concentration, all fits intersected at the same Z_{DHH} of ∼2.6. Furthermore, D_m at this intersection (∼4.4×10^{-7} cm^2/s) corresponds to the self-diffusion, D_s, value observed in Figure 2A and B and agrees with previous determinations of D_s [7]. Figure 3B highlights the explicit relationship between the k_D and Z_{DHH}. It is striking that moving left to right across the x-axis, k_D switches from net attraction ($k_D < -5.34$ mL/g) to net repulsion ($k_D > 0$) at $Z_{DHH} < 5$. The blue dashed line in Figure 3B identifies that the k_T and k_H contributions to k_D are equivalent ($k_D = 0$ mL/g). The red dashed line indicates the k_D

predicted by Yadav *et al.* where there are no net attractive or repulsive protein–protein interactions ($k_D < -5.34$ mL/g) [7]. Thus, the pink shaded area in Figure 3A and B shows the Z_{DHH} region where protein–protein interactions switch from attractive (below the red dashed line) to repulsive (above the red dashed line). Though the critical Z_{DHH} range might be better defined using more mAbs, the fact that IgGs exhibit weak attractive interactions of varying strength [19] ($K_{d\text{-apparent}} > 100\ \mu M$) makes it difficult to say whether this range would be broader or narrower. In any case, the implications of this result are intriguing.

DISCUSSION

For the first time we use measurements to identify a Z_{DHH} range where the thermodynamic and hydrodynamic contributions to k_D balance. In the absence of thermodynamic interactions, $k_T = B_{22} = 0$ (indicating no net attractive or repulsive interactions). Under these conditions only k_H, the hydrodynamic contribution to k_D, remains. It has been estimated that IgGs should exhibit k_D values of either −5.34 mL/g[7] or − 8.0 mL/g [21] under these conditions. Kholodenko and Douglas predict that k_D should equal the negative intrinsic viscosity [η_i], or − 2.5 mL/g for non-interacting spheres [22, 23]. However, [η_i] is sensitive to shape [24]. For mAbs, which have an axial ratio ∼ 5, both the measured and predicted value of [η_i] are ∼6 mL/g [24, 25], resulting in $k_H = -6$ mL/g, which is in excellent agreement with the Yadav *et al*. prediction of −5.34 mL/g [5].

The data in Figure 3A were fit to a general logarithmic function simply to guide the eye and show the trend of the diffusion data, with no theoretical justification. At this time, the fact that the lines in Figure 3A all cross at the same value as D_s (D_m extrapolated to zero protein concentration) must be considered an intriguing observation. Furthermore, for the first time we report the Z_{DHH} range over which the interactions contributing to the k_D go from net attractive to net repulsive, giving an indication the *minimum* mAb surface charge is needed for good solubility and low viscosity. It must be kept in mind, however, that greater Z_{DHH} may be needed to overcome the intrinsic attractive interactions between IgGs [19].

CONCLUSION

This brief report highlights a novel methodology that may be used to improve mAb screening assessments, by being able to differentiate within candidates that have physical stability attributes dominated by electrostatic conditions and appear not to strongly self-associate at the solvent conditions used. Although some surface charge on a molecule might be good to prevent aggregation [26], non-uniform distribution of charge across the molecule can cause dipoles that have adverse effects on high concentration properties such as solution viscosity [16] and solubility [27]. This result may provide a starting point to identify the minimum amount of charge desired on the surface of mAb candidates to guide earlier protein design and engineering decisions.

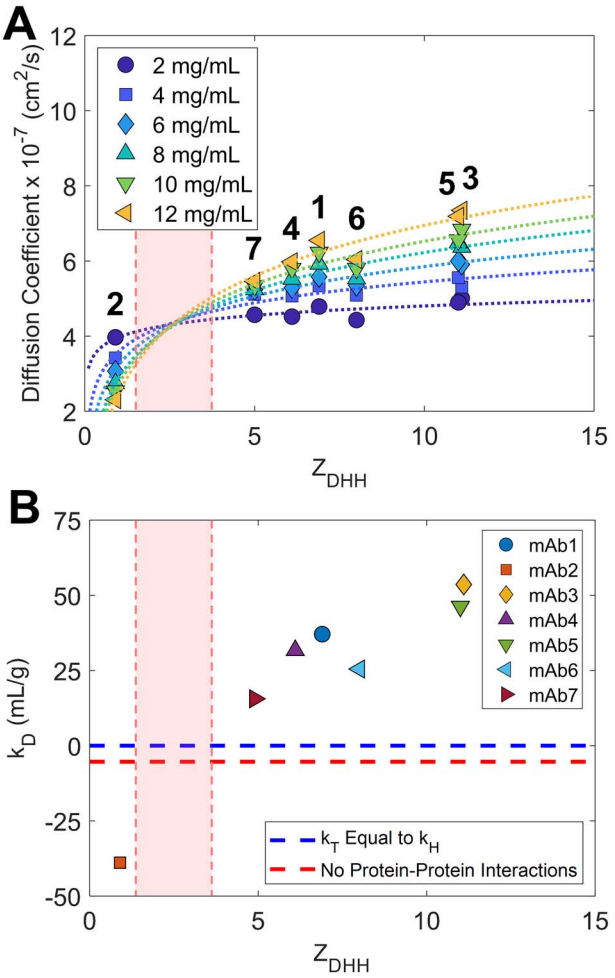

Figure 3. Protein concentration and diffusion coefficient data plotted versus surface charge. (A) The diffusion coefficient for the seven mAbs in 15 mM histidine buffer, pH 6 plotted as a function of ZDHH at various protein concentrations. The dotted lines are general logarithmic model fits to the data (Dm = a*ln(b*ZDHH), where a and b are the constants) are to guide the eye and all have R^2 values above 0.97. Each vertical grouping of data points at constant ZDHH corresponds to a different mAb identified by the numeral above the data grouping, consistent with the mAb numbering in Figures 1 and 2. Note that mAb3 and mAb5 both had a ZDHH of ∼11. (B) The kD is a more conventional representation of the protein concentration and diffusion coefficient data shown in panel A as a way to understand protein interactions in solution. The kD was measured at 15 mM histidine, pH 6, and plotted against ZDHH. The horizontal blue dashed line represents the point at which thermodynamic and hydrodynamic interactions contribute equivalently to the kD, and the horizontal red dashed line represents the kD of ∼ −5.34 mL/g that represents no attractive or repulsive interactions between IgG proteins. 14 The pink shaded area between the vertical pink dashed lines shows the ZDHH regime in which the kD inflection point happens as it goes from attractive to repulsive.

FUNDING STATEMENT

This research was funded by AbbVie Inc.

DATA AVAILABILITY STATEMENT

The design, study conduct, and financial support for this research were provided by AbbVie. AbbVie participated

in the interpretation of data, review, and approval of the publication.

CONFLICT OF INTEREST STATEMENT

The authors declare no conflict of interest and may own AbbVie stock. Dana Filoti is an employee of AbbVie. Thomas M. Laue is a Carpenter Emeritus Professor at the University of New Hampshire. Joshua Laber is currently an employee of Nektar Therapeutics.

ETHICS AND CONSENT

This work has been conducted by respecting the ethical scientific standards.

ACKNOWLEDGEMENTS

The authors would like to thank Czeslaw Radziejewski for critical review of this manuscript and to Dorth Korst for management and support of this work through the AbbVie Postdoctoral Program.

ANIMAL RESEARCH

No applicable. No animals have been used for conducting this research.

REFERENCES

1. Blanco, MA, Sahin, E, Li, Y *et al.* Reexamining protein–protein and protein–solvent interactions from Kirkwood-Buff analysis of light scattering in multi-component solutions. *J Chem Phys* 2011; **134**: 225103-225101–12.
2. Hung, JJ, Dear, BJ, Karouta, CA *et al.* protein–protein interactions of highly concentrated monoclonal antibody solutions via static light scattering and influence on the viscosity. *J Phys Chem B* 2019; **123**: 739–55.
3. Yadav, S, Shire, SJ, Kalonia, DS. Viscosity analysis of high concentration bovine serum albumin aqueous solutions. *Pharm Res* 2011; **28**: 1973–83.
4. Woldeyes, MA, Calero-Rubio, C, Furst, EM *et al.* Predicting protein interactions of concentrated globular protein solutions using colloidal models. *J Phys Chem B* 2017; **121**: 4756–67.
5. Curtis, RA, Prausnitz, JM, Blanch, HW. Protein-protein and protein-salt interactions in aqueous protein solutions containing concentrated electrolytes. *Biotechnol Bioeng* 1998; **57**: 11–21.
6. Ruppert, S, Sandler, SI, Lenhoff, AM. Correlation between the osmotic second virial coefficient and the solubility of proteins. *Biotechnol Prog* 2001; **17**: 182–7.
7. Yadav, S, Shire, SJ, Kalonia, DS. Factors affecting the viscosity in high concentration solutions of different monoclonal antibodies. *J Pharm Sci* 2010; **99**: 4812–29.
8. Connolly, BD, Petry, C, Yadav, S *et al.* Weak interactions govern the viscosity of concentrated antibody solutions: high-throughput analysis using the diffusion interaction parameter. *Biophys J* 2012; **103**: 69–78.
9. Shi, S, Uchida, M, Cheung, JK *et al.* Method qualification and application of diffusion interaction parameter and virial coefficient. *Int J Biol Macromol* 2013; **62**: 487–93.
10. Lehermayr, C, Mahler, H-C, Mäder, K *et al.* Assessment of net charge and protein–protein interactions of different monoclonal antibodies. *J Pharm Sci* 2011; **100**: 2551–62.
11. Laue, TM. Proximity energies: a framework for understanding concentrated solutions. *J Mol Recognit* 2012; **25**: 165–73.
12. Laue, TM, Shire, SJ. The molecular interaction process. *J Pharm Sci* 2020; **109**: 154–60.
13. Tomar, DS, Singh, SK, Li, L *et al.* In silico prediction of diffusion interaction parameter (kD), a key indicator of antibody solution behaviors. *Pharm Res* 2018; **35**: 1–20.
14. Neal, BL, Asthagiri, D, Lenhoff, AM. Molecular origins of osmotic second virial coefficients of proteins. *Biophys J* 1998; **75**: 2469–77.
15. Filoti, DI, Shire, SJ, Yadav, S *et al.* Comparative study of analytical techniques for determining protein charge. *J Pharm Sci* 2015; **104**: 2123–31.
16. Yadav, S, Laue, TM, Kalonia, DS *et al.* The influence of charge distribution on self-association and viscosity behavior of monoclonal antibody solutions. *Mol Pharm* 2012; **9**: 791–802.
17. Yang, D, Kroe-Barrett, R, Singh, S *et al.* IgG charge: practical and biological implications. *Antibodies* 2019; **8**: 24.
18. Jr, S, de Jong, RN, Beurskens, FJ *et al.* Weak fragment crystallizable (Fc) domain interactions drive the dynamic assembly of IgG oligomers upon antigen recognition. *ACS Nano* 2020; **14**: 2739–50.
19. Yang, D, Correia, JJ, Stafford, WF III *et al.* Weak IgG self- and hetero-association characterized by fluorescence analytical ultracentrifugation. *Protein Sci* 2018; **27**: 1334–48.
20. Velev, OD, Kaler, EW, Lenhoff, AM. Protein interactions in solution characterized by light and neutron scattering: comparison of lysozyme and chymotrypsinogen. *Biophys J* 1998; **75**: 2682–97.
21. Jayaraman, J, Wu, J, Brunelle, MC *et al.* Plasmonic measurements of monoclonal antibody self-association using self-interaction nanoparticle spectroscopy. *Biotechnol Bioeng* 2014; **111**: 1513–20.
22. Kholodenko, AL, Douglas, JF. Generalized stokes-Einstein equation for spherical particle suspensions. *Physical Review E* 1995; **51**: 1081–90.
23. Douglas, JF, Curtis, RA, Sarangapani, PS *et al.* Hard spheres with purely repulsive interactions have positive diffusion interaction parameter, kD. *Biophys J* 2017; **113**: 753–4.
24. Douglas, JF, Garboczi, EJ. Intrinsic viscosity and the polarizability of particles having a wide range of Shapes. *Adv Chem Phys* 1995; 85–153.
25. Pindrus, MA, Shire, SJ, Yadav, S *et al.* The effect of low ionic strength on diffusion and viscosity of monoclonal antibodies. *Mol Pharm* 2018; **15**: 3133–42.
26. Kumar, V, Dixit, N, Zhou, LL *et al.* Impact of short range hydrophobic interactions and long range electrostatic forces on the aggregation kinetics of a monoclonal antibody and a dual-variable domain immunoglobulin at low and high concentrations. *Int J Pharm* 2011; **421**: 82–93.
27. Laber, JR, Dear, BJ, Martins, ML *et al.* Charge shielding prevents aggregation of supercharged GFP variants at high protein concentration. *Mol Pharm* 2017; **14**: 3269–80.